

Highly mismatched antiferroelectric films: Transition order and mechanical state

Maria A. Kniazeva^{1,*}, Alexander E. Ganzha¹, Ran Gao,² Arvind Dasgupta,²
 Alexey V. Filimonov¹ and Roman G. Burkovsky^{1,†}

¹*Institute of Electronics and Telecommunications, Peter the Great Saint-Petersburg Polytechnic University,
 29 Politekhnicheskaya, 195251, St. Petersburg, Russia*

²*Department of Materials Science and Engineering, University of California, Berkeley, California 94720, USA*



(Received 21 January 2023; revised 14 April 2023; accepted 26 April 2023; published 22 May 2023)

Epitaxial $\text{PbZrO}_3/\text{SrRuO}_3/\text{SrTiO}_3$ heterostructures are among the most widely studied thin-film antiferroelectrics. This paper explores their temperature-induced phase transitions and the characteristics of the domain structure by means of high-resolution synchrotron x-ray diffraction. The antiferroelectric transition order appears to change from the first to the second; peculiar in-plane M -point superstructures develop at high temperatures, manifesting a new phase; the R - and Σ -point superstructure reflections demonstrate much reduced splitting as compared to the demands of the mechanical compatibility. We discuss the energetics of the reduced around-the-normal antiferroelectric domain tilts, its relation to the observed changes in phase transitions, and point to the possible contribution to the observed effect from an unusual diffraction mechanism related to the partial coherence between domains in a random nanodomain structure.

DOI: [10.1103/PhysRevB.107.184113](https://doi.org/10.1103/PhysRevB.107.184113)

I. INTRODUCTION

Epitaxial heterostructures can be ideally matched, strained, or relaxed. The matched and strained structures can be, in principle, defect-free, while the relaxed are essentially defectful because of strain-relaxing dislocations [1]. All three types are useful in technology [2]. Commonly, the relaxed heterostructures are understood as an unavoidable evil in doing epitaxy with lattice-mismatched materials. However, one can expect the possibility of using the relaxation constructively, in a form of defect engineering [3,4].

An example where that might be at play is $\text{PbZrO}_3/\text{SrRuO}_3/\text{SrTiO}_3$ antiferroelectric heterostructures, in which some of us have recently observed field-induced heterophase states that are unlikely to form without defect-induced spatial heterogeneity of the material [5]. That finding, together with overall high attention to PbZrO_3 material as a model antiferroelectric [6–8] and a similar emerging status for this film-substrate combination [9–12] calls for a systematic study of phase transitions in it. In particular, it deems desirable to learn about how the peculiarities of the transitions in relaxed thin-film form are linked to the mechanical state of the material.

The mechanical state here implies few aspects. First, it is the single-domain strain, as considered in theoretical works [13–15]. Second, it is the strain related to polydomainness and possibly heterophasy, as in Refs. [16,17]. Third, it is the effects related specifically to relaxation [18], like those in Refs. [19,20].

Experimentally, the mechanical state of $\text{PbZrO}_3/\text{SrRuO}_3/\text{SrTiO}_3$ has been studied by few groups, which agree that the dominating share of the film volume experiences very small [21] or negligible [11,12] average strain, i.e., is nearly completely relaxed. This suggests that the modifications to temperature-induced phase transitions, as found in Refs. [11,12,22], are likely due to the effects other than average strain.

The most notable of those modifications, as compared to the bulk, are the shift of the dielectric maximum towards higher temperatures [11,12], which implies a higher temperature of losing the symmetry of the high-temperature phase, the appearance of new superstructural reflections at about those high temperatures, and a surprisingly linear temperature trend of the antiferroelectric reflections [22].

In this paper, we use synchrotron x-ray diffraction to probe the mechanical state as evidenced by reflection broadening and emergent splitting and, at the same time, monitor the phase transitions by inspecting the superstructural intensities. The mechanical compatibility of antiferroelectric domain configuration appears considerably compromised in favor of minimizing the material microtwists near the interface, which implies a considerable intra-domain strain that can influence the material behavior. The behavior, in turn, is influenced rather dramatically. We discover a separation between the temperatures at which the antiferroelectric and octahedral-tilting distortions develop, which contributes to mounting evidence towards a change of the transition order from the first to the second.

The strain characterization methodology, which is based on reflection splitting, being a potentially very powerful tool in studying ferroics, also has its nontrivial subtleties, such as a potential complication of the signal by the interdomain

*kniazeva.maria225@yandex.ru

†roman.burkovsky@gmail.com

TABLE I. Summary of the observed superstructural reflections and possible corresponding distortions. Modes that correspond to Zr displacements and octahedral group distortions are not shown because they are unlikely to occur in such crystals.

Point and (h, k, l)	Condition	Possible distortions
$R (H + \frac{1}{2}, K + \frac{1}{2}, L + \frac{1}{2})$	$ h = k = l $ none	R_5^+ mode, lead ion displacements Same or R_4^+ mode, antiphase tilts of O_6 groups
$M (H + \frac{1}{2}, K + \frac{1}{2}, L)$	$ h = k $ none	M_5^- mode, lead ion displacements Same or M_3^+ mode, in-phase tilts of O_6 groups
$\Sigma (H + \frac{1}{4}, K + \frac{1}{4}, L)$	none	Σ_2 mode, transverse lead ion displacement wave, which propagates along $[1\ 1\ 0]$ and is polarized along $[1\ -1\ 0]$, accompanied by oxygen sublattice distortion
$\Sigma_1 (H + 0.15, K + 0.15, L)$	none	Same, but with larger period

coherence, when the domains are very small. We discuss that implication on the understanding of the results.

II. METHODS

A. Samples

The samples were 100- and 50-nm-thick (001)-oriented epitaxial films of $PbZrO_3$ grown on a $SrTiO_3$ substrate with an intermediate $SrRuO_3$ layer. Synthesis has been done by pulsed laser deposition at UC Berkeley, as in Refs. [5,22,23]. This paper is focused on the results obtained with 100-nm film, the data for 50-nm film has been partially published [22] and are added here for comparison.

B. X-ray diffraction

The measurements were made on the ID03 beam-line of the European Synchrotron Radiation Facility (ESRF). The samples were put in the vacuum chamber, where they were resistively heated. The measurements were carried out in the cooling mode in a temperature range from $T = 370^\circ\text{C}$ to 110°C . The wavelength of the x-ray beam was $0.517\ \text{\AA}$. Angular positioning was done using a six-circle goniometer, which allowed us to perform all the measurements with a single angle of incidence. We have chosen this angle as 0.13° , where the signal intensity was found to be optimal. Superstructure reflection positions and their possible origins are summarized in Table I.

C. Computing split Bragg positions

There is an expectation for single-crystal samples that the domain structure is organized so each domain experiences zero stress, which is referred to as the mechanical compatibility requirement [1]. This requirement determines the orientation of domain walls and also the angles by which the domains need to tilt with respect to each other to maintain the material cohesion [Fig. 1(a)]. Those angles and spontaneous strain can predict the positions of splitted reflections. We use such a single-crystal prediction as a reference for analyzing the splitting in films.

We note that $PbZrO_3$ is pseudotetragonal with respect to its spontaneous strain [24]. The pseudotetragonal lattice parameters are computed as $a_{pt} = a_o/\sqrt{2} \approx b_o/(2\sqrt{2})$, $c_{pt} = c_o/2$, where the o -subscripted constants are those of the orthorhombic

cell [25,26]. The relationship between the orthorhombic and pseudotetragonal cells is shown in Fig. 1(d). The antiferroelectric (AFE) domains in experiment are those with the shorter c_{pt} parallel to the film surface [22]. In a stress-free configuration, those need to be separated by 90° domain walls, as depicted in Fig. 1(b), forming the series of stripe domains. There are two variants of those series, which are different in the tilt direction for a particular domain orientation. The domain tilt angles, ϕ , are determined as [1] $2\phi = |\Delta c - \Delta a|/a_c$, where a_c is a cubic lattice constant, $\Delta c = c_{pt} - a_c$, $\Delta a = a_{pt} - a_c$. The angle 2ϕ is referred to as clapping angle [6]. The value of a_c can be defined as convenient, so we take it as $(a_{pt} + c_{pt})/2$, making $|\Delta c| = \Delta a$.

The difference between the pseudocubic reflection position and the splitted position is calculated in two steps. First, the scattering vector, $\vec{Q} = (h, k, l)$, is scaled according to the spontaneous strain tensor, and then it is rotated by ϕ . It is straightforward to obtain that the resulting wave-vector shift, $\Delta\vec{Q}$, is expressed rather simply like $(h - k, h - k, 0)\frac{\Delta a}{a_c}$ for point 1 in Fig. 1(c). In the calculations, we took the spontaneous strains for different temperatures from Whatmore and Glazer [24].

Generally, there shall be four split positions, but some of them can have zero intensity. For example, only two positions can be observable for the Σ reflections.

III. RESULTS

A. Superstructure intensities and a possibility of transition order change

1. Linear trend for Σ reflections

The intensities of the various reflections exhibit several unexpected properties (Fig. 2). The first, and perhaps most important, is that there is no abrupt appearance of Σ superstructures, as in single crystals. In films, Σ superstructures appear gradually, without apparent breaks, although at approximately the same temperature as in single crystals. First in mind is the change of transition type from first order (as in single crystals [24,25]) to second order. Theoretically, such a change of transition type is possible during the transition from the bulk to the film, which was widely discussed in theoretical works on ferroelectric films [13,16,18]. During the second-order transition, the intensity of the superstructures would have to be linear in temperature since it is proportional

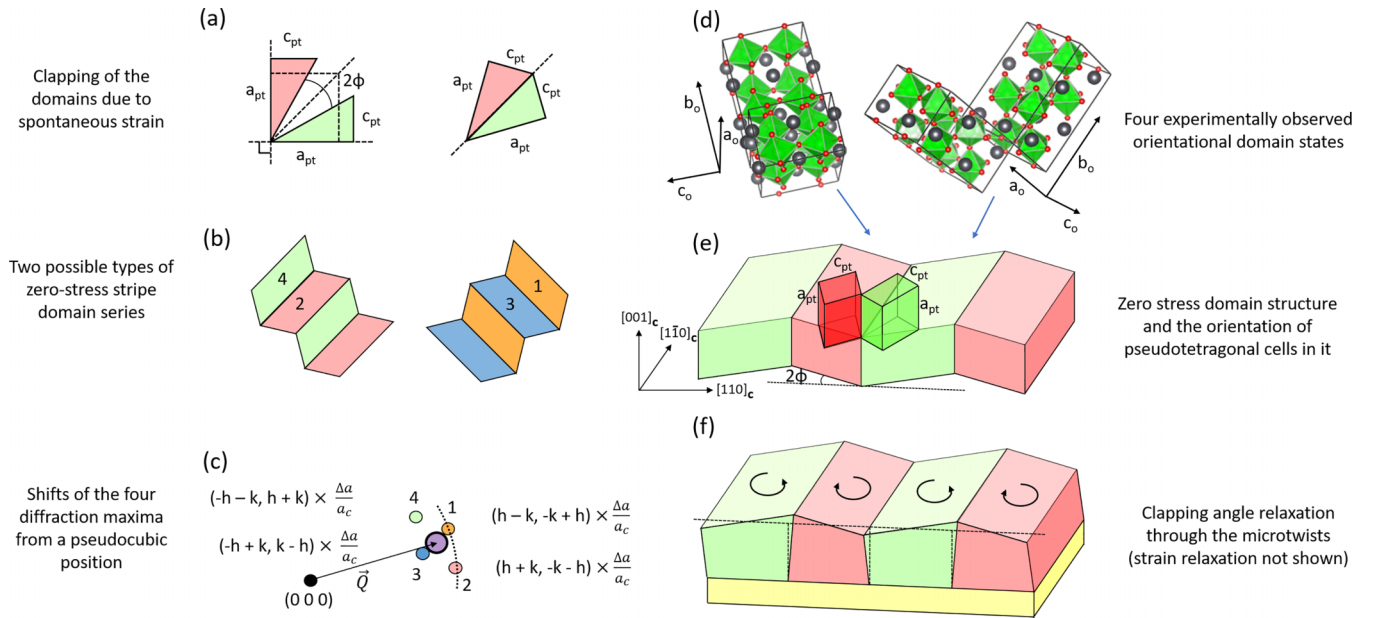


FIG. 1. Scheme of idealized zero-stress domain clapping and its relation to the experiment. (a)–(c) show how clapping should work in the case of ideal tetragonal domains, which domain series should arise, and how that should result in Bragg reflection splitting. (d)–(f) show how the real orthorhombic PbZrO_3 cell relates to the above idealized tetragonal cell and how the respective domain tilts need to be relaxed through microtwists upon approaching the substrate.

to the square of the order parameter, which behaves like the square root of the temperature difference $T_0 - T$ [27]. The experimental dependence of the Σ points appears as such a straight line. Taking the change from the first-order to second-order transition as a working version, let us turn to the related observations.

2. Separation of Σ and R superstructure formation temperatures

The separation of the formation temperatures of Σ ($\sim 210^\circ\text{C}$) and R superstructures ($\sim 235^\circ\text{C}$), which is most clearly seen from the plot by stars in Fig. 2(c), testifies in favor of the second-order transition. The difference is small (about 25°C) but seems to be quite reliable, since the measurements of different superstructures were done in a single temperature cycle. If there were no such separation, the scenario of the second-order transition would hardly be feasible because the two types of distortions corresponding to different points of the Brillouin zone cannot be formed at once in a second-order transition. When the antiphase tilts of the oxygen octahedra form before the lead displacements, the lead displacements can form by a second-order transition. A similar situation likely occurs in $\text{PbHfO}_3\text{--PbSnO}_3$ [28] single crystals, where a low-symmetry *intermediate* phase with *Imma* structure without lead waves (incommensurate or AFE) is formed first by creating tilts and then the lead displacements are formed through a critical increase in the incommensurate susceptibility.

The analogy above may be useful but it is not entirely direct, since the situation is further complicated in films. In particular, simultaneously with the tilts ($T \sim 235^\circ\text{C}$), incommensurate waves are formed at Σ_1 points, for which the modulation vector is $\vec{q} = (h \pm 0.15, 0, l \pm 0.15)$. Their intensity is an order of magnitude lower than the intensity of Σ

superstructures [Fig. 2(b)]. Most likely, the Σ_1 superstructure is realized in a very limited volume of the sample (see estimate in the section related to M point), possibly near the interface, where strong changes in properties are expected, leaving the rest of the film volume free for the implementation of the second-order scenario for the AFE distortion.

The delayed formation of AFE waves compared to the tilts also manifests itself at low temperatures, where the ratio of the intensities of the Σ and R reflections is approximately two times lower than it should be in the bulk [see Fig. 2(c)]. Calculation of this ratio according to the well-known structure [25] (we used the VESTA program to calculate the structure factors), taking into account that the Σ reflection comes from only one domain orientation and the R reflection sums the intensities from the four different equivalently populated orientations, predicts a difference of approximately five times. From the experiment, we see about 2.5 times for both films. That is, the Σ reflections turn out to be two times weaker than it would be if the structure of each of the AFE domains was equivalent to bulk PbZrO_3 .

We see the most constructive interpretation of this observation as the anomalously large Debye-Waller factor for lead ions, which arises as a result of their greater disordering compared to the bulk, and the large imperfection of the modulation wave. This is also compatible with the idea of a delay of the second-order AFE transition after the formation of tilts if we assume that the AFE order parameter characterizes not the magnitude of the displacements but their ordering, as recently shown by first-principles modeling for the bulk PbZrO_3 [29].

As for the comparison of intensities with those in the bulk, it is worthy to note a decently seen symmetric $(0.5 \ 0.5 \ 0.5)$ R -point reflection. It cannot come from tilts [30] by symmetry.

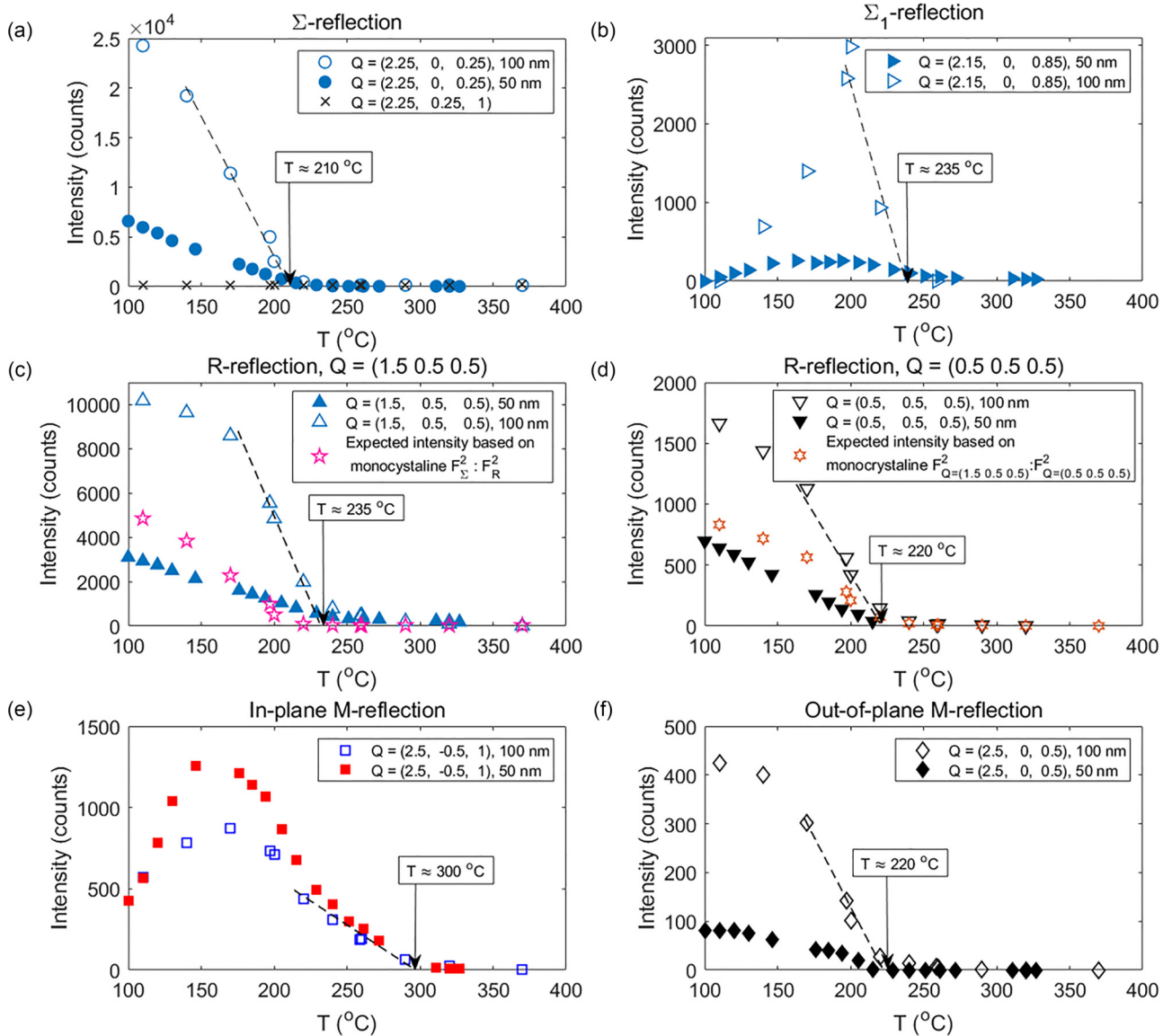


FIG. 2. Temperature dependence of superstructures in 100- and 50-nm PbZrO_3 films on $\text{SrRuO}_3/\text{SrTiO}_3$. Stars in the R -reflection plots show their expected intensity, as recalculated from Σ intensity and the single-crystal structure factor ratios (see text). R reflections begin to grow earlier on cooling. Also note the linear trend for Σ reflections, the presence of symmetric R reflection, and the appearance of M reflections at much higher temperatures than Σ -reflections.

In the solved structure, as represented by CIF files of Corker *et al.* [26] and Fujishita and Hoshino [25], this reflection comes mainly from the minor R_5^+ distortion mode. This is likely the origin of this reflection in films.

3. M -point superstructure

Surprisingly, even above the tilt (R -reflection) formation temperature, the film already contains superstructures at the M points, which appear at about 300°C and extend deep into the region of existence of the AFE phase, having a maximum around 170°C . It seems very probable that the corresponding superstructure is also realized in very small volumes, since the reflections at the M points, as well as the Σ_1 points, are an order of magnitude weaker than Σ and R superstructures.

It is not possible to find whether they are in a cubic matrix or some other one from diffraction. It should be noted that in similar samples of Gao *et al.* [11] and Si *et al.* [12], a fairly clear maximum is observed in the dielectric permittivity in the region of 270 – 280°C , below which a monotonous decrease in susceptibility occurs.

If the present M superstructures can correlate with a similar maximum, we can assume that small volumes of the M superstructure are not in the cubic but in some low-symmetry phase, the transition to which accompanies the high-temperature maximum of the susceptibility. Among the candidates known from the literature for such a noncubic host phase, the rhombohedral phase proposed by Ricote *et al.* [31] for low-titanium $\text{Pb}(\text{Zr-Ti})\text{O}_3$ seems to be the closest. Its peculiarity lies precisely in the fact that, despite the rhombohedral structure

of the average structure, there are M -type reflections that are incompatible with this average structure, and therefore originate from inclusions. The material used by Ricote *et al.* is very close to PbZrO_3 , differing by a small doping with titanium atoms, so the structure observed in it can also be expected under other perturbations of PbZrO_3 , for example, upon integration into films, as here.

A feature of inclusions with the M superstructure is that at high temperatures they are formed only with the reduced wave vector parallel to the film surface. This differs it from AFE and incommensurate structures, which have modulation vectors away from the film surface. For the AFE phase that occurs because of the specifics of its spontaneous strain tensor, where the material is compressed along the orthorhombic c axis. To maximally squeeze the domain structure in the film's plane, as the lattice mismatch with the substrate demands, only those domains are formed where the c axis is along the surface. This results in AFE modulation being out of film's plane. The fact that M -superstructure inclusions follow the opposite rule suggests that their structure has different relationship between spontaneous strain and modulation direction, as compared to the AFE and incommensurate phases.

The domains with the M superstructure themselves should have an orthorhombic or monoclinic cell, but not a rhombohedral one. Although, formally, an M -point superstructure can be compatible with a rather large rhombohedral cell (Ricote *et al.* [31] disagree), for example, the $R3m$ group with basis $(2, 0, -2)$, $(0, -2, 2)$, $(-1, -1, -1)$ in pseudocubic coordinates, rhombohedral symmetry would lead to the simultaneous observation of M reflections with wave vectors parallel and nonparallel to the film surface. This contradicts the observations. The simplest variant of a cell that satisfies observations is a cell built on the vectors $(a\sqrt{2}, a\sqrt{2}, 0)$, $(a\sqrt{2}, -a\sqrt{2}, 0)$, $(0, 0, a)$, where a is the pseudocubic lattice constant. Theoretically, the displacements of ions in this cell could be antiphase shifts of lead ions, as considered by An *et al.* [32] or in-phase tilts of octahedrons in the $a^0a^0c^+$ pattern, as suggested by Viehland *et al.* [33] for $\text{Pb}(\text{Zr-Ti})\text{O}_3$.

Almost certainly, the displacements are of lead ions and not of oxygen ions. We deduce that from the estimated volumes of different phases. Relative volumes can be estimated by dividing intensities by respective squared structure factors. We did such calculations using structure factors computed by VESTA software on the basis of manually constructed CIF files for hypothetical structures (only the AFE structure is known from crystallography [25,26]). When taking the volume of the AFE phase at 110°C as unity, the remaining relative volumes are as follows. The incommensurate phase in its maximum at 200°C occupies a relative volume of about 0.13. The relative volume that produces an in-plane M superstructure is 0.01 if we assume antiparallel lead ion shifts as its origin and 2.3 if we assume that it comes from in-phase octahedral tilts by about 10° around normal. It is totally unlikely that the in-phase tilted structure at about 170°C occupies 2.3 times larger volume than the AFE structure at 110°C . If that was the case, one would expect a strong dip in Σ -point temperature dependence where the M point peaks. Therefore, it is almost certain that the in-plane M points come from antiparallel lead ion displacements.

B. Shapes and broadening of reflections

1. Overview

Three types of broadening are observed. First, the broadening of Σ reflections due to antiphase domain walls, which is similar to that in single crystals. Second, the broadening of Σ and R reflections, which is expected from the domain clapping to obey the mechanical compatibility requirements. Third, the broadening of the in-plane M reflections, which is, apparently, governed by something else. Visual material is in Fig. 3.

2. Broadening of Σ reflections due to antiphase domains and walls

This is the broadening of Σ reflections along the modulation wave vector, as observed in the $H - L$ planes for AFE [Fig. 3(a)] and incommensurate [Fig. 3(b)] reflections. The origins of such a broadening are the breaks in the phase, ϕ , of the modulation wave. In the case of AFE domains, those breaks correspond to the antiphase domain walls, which separate domains with the same orientational states but different translational states. Such walls are oriented perpendicularly to the modulation wave vector, so producing the scattering along that wave vector. In single crystals, it appears possible to distinguish straightforwardly between the Bragg reflection broadening in that direction and the diffuse scattering rod along the same direction [34]. The former characterizes the widths of domains, while the latter is expected to characterize the widths of the walls themselves. In films, this effect appears similarly, although the broadening of the peak is not straightforwardly distinguishable from diffuse scattering.

3. Incomplete splitting of reflections due to domain clapping

Only those AFE domains are present, for which the c axis is along the film surface. Therefore, the domains with the c axis along H need to connect with the domains with the c axis along K . If the sample was a free-standing film, such a domain connection would be possible without mechanical stresses in two distinct configurations, as specified in Sec. IIC above. Generally, each pseudocubic reflection should split into four different pseudotetragonal reflections, each corresponding to a specific combination of spontaneous strain and domain tilt. A splitting of similar origin has been recently reported by Oliveira *et al.* in NaNbO_3 epitaxial films [35]. The positions where the splitted reflections should be observed for stress-free PbZrO_3 are marked by black circles in the respective plots for Σ -, R -, and out-of-plane M -reflections.

The observations both agree and disagree with the prediction.

The agreement is in that the reflections broaden in the $H - K$ plane and do not broaden along the L direction, which is compatible with the predicted domain tilting along L . The reflections broaden more for larger scattering vectors, which is also expected because the difference in strain and tilt should work this way, as contrasted to the wave-vector-independent broadening due to domain sizes [36].

The disagreement is that instead of the four (or two in the case of Σ reflections) separate peaks, we observe one peak that is broadened as if it wanted to split as expected but does not. This cannot be ascribed to the merging of correctly

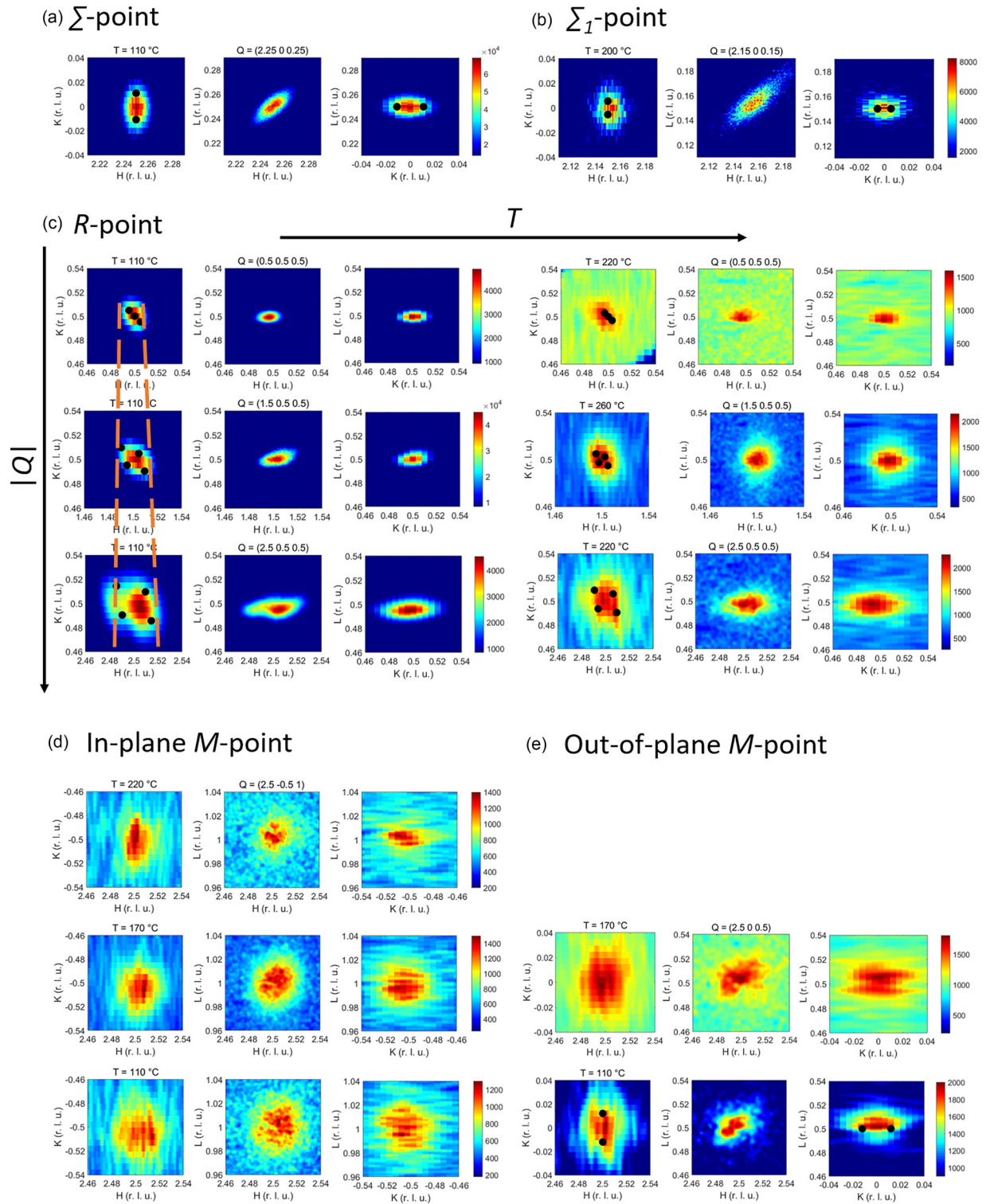


FIG. 3. Representative superstructures in 100-nm $\text{PbZrO}_3/\text{SrRuO}_3/\text{SrTiO}_3$. Black circles show the positions of reflections for the case of full mechanical compatibility of the antiferroelectric domains in the free-standing material.

positioned peaks due to their finite sizes, as the intensity distribution is concentrated between the theoretical points and ends just outside the range demarcated by points, as seen most clearly for Σ reflection and low-temperature and large-wave-vector R reflection. The distributions just touch the theoretical points.

The zero-stress theoretical model is clearly relevant to the observations but is also obviously insufficient.

Notably, the out-of-plane M peak follows the same broadening pattern as the R and Σ peaks do. That suggests the same relationship between its modulation vector direction and the spontaneous strain so its cell can be organized similarly.

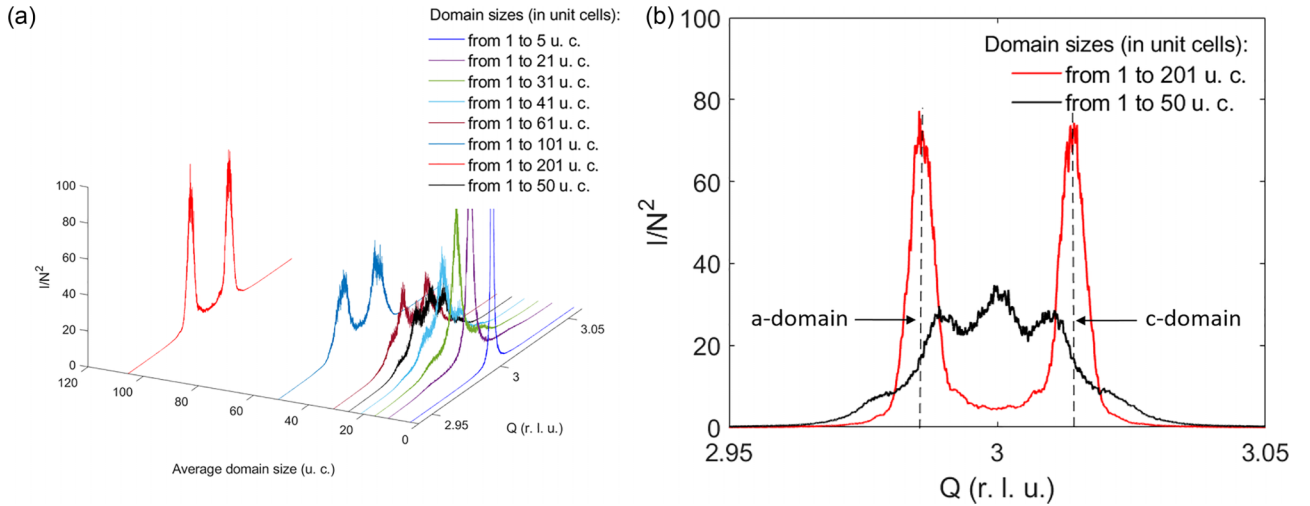


FIG. 4. Simulated diffraction at one-dimensional point scatterer chains that are analogous to those in stripe AFE domain structures. Each chain consists of alternating blocks having interatomic distance of either 4.11 Å or 4.15 Å. Each chain is characterized by its average domain size. Scattering profiles change qualitatively with that parameter.

4. In-plane M reflections are different at low temperatures

At high temperatures, where the AFE modulations are absent, the in-plane M reflection is broadened similarly to the Σ reflection, elongated as if due to around-the-normal domain tilting. However, when the temperature goes down, those reflections become broadened isotropically. It is difficult to imagine how the strain-plus-tilt broadening, as discussed above, could produce such. Tentatively, such an isotropic broadening can arise when the particles producing them become small and isotropic, which might well occur as the M superstructure loses volume to the rapidly developing AFE superstructure on cooling.

5. Possible limited interdomain coherence effect

The absence of the expected reflection splitting suggests that the spontaneous strains are smaller than in single crystals or that the mechanical compatibility is somehow compromised.

However, we are cautious towards such an indication, and check whether this could be a peculiarity of diffraction in nanodomain structures. Indeed, it is known that regular nanodomain structures can cancel the peaks from the lattices of individual domains and create peaks that do not correspond to any of the lattices [37]. We ask whether a similar effect can produce intensity cusps distributed between the expected peak positions, similarly to what we observe in Fig. 3.

To check that we have simulated the diffraction from one-dimensional chains of scattering centers that are analogous to a nanodomain structure with alternating domains, with $a_{pt} = 4.15$ Å and $c_{pt} = 4.11$ Å lattice spacings, respectively, for each chain, we chose the domain sizes to be random with a flat distribution from just one cell to $2d$, where d is the characteristic domain size of the chain. Intensity was computed according to the standard formula $I(\vec{Q}) = |\sum_i \exp(i\vec{Q}\vec{r}_i)|^2$, averaged over many random incarnations.

There are different scattering regimes (Fig. 4). When the domains are large, they scatter independently and we see the two peaks corresponding to the two lattice spacings, a_{pt} and

c_{pt} . When the domains are small, the chain diffracts as if there was an average lattice with spacing $(a_{pt} + c_{pt})/2$, a single sharp peak is observed instead of two. At intermediate sizes, there is a crossover between those two diffraction regimes, where an intensity cusp is observed.

Interestingly, such a cusp is organized so its intensity drops at about the same position, where the large-domain peak would reside, similarly to the experimental intensity decaying at about the positions predicted by zero-stress theory. These simulation results should be considered as an insight, since many factors need to be taken into account for an accurate conclusion, as we discuss below.

IV. DISCUSSION

The most captivating observations are the apparent change of the AFE transition order, as evidenced by linear temperature dependence of Σ reflections, and that the antiferroelectric domain structure does not show the reflection splitting as it has to show according to the material structure.

A. Transition order change

The transition order change is difficult to prove independently, as the AFE order parameter is not linked to the macroscopically measurable susceptibility, such as dielectric permittivity, and the calorimetric measurements in films are of great difficulty [38]. A possibility of validating the second order of the transition exists, in principle, upon measuring the AFE or incommensurate susceptibility by diffuse and inelastic scattering, as done in single crystals [28,39–43]. For films, this methodology has not yet been applied. If confirmed in the present films, this phenomenon would be of interest for theoretical analysis, where epitaxial engineering of the transition orders in ferroelectrics has attracted considerable interest [13]. If not, it prompts interest in what drives such a continuous increase of AFE intensity, and whether and how it can be linked to the extrinsic (outside of domain) effects, such as gradual consumption of one phase by another.

B. Absence of reflection splitting

The fact that reflections do not split as expected is also a delicate one. The clapping angles and, consequently, the reflection splitting are totally defined by the strains in the material, which include spontaneous strains due to the interaction with the order parameter, and also strains due to the external sources, such as elastic interactions between different domains and those with the substrate. Working along this line of thought, one needs to assume that the total strains in the domains are considerably smaller than the spontaneous strains; this way the splitting might be, in principle, reduced to the observed level. Which external stresses can work so effectively against the spontaneous strains?

An obvious option seems to be the epitaxial stress due to the contact with substrate. This stress is compressive because both the pseudotetragonal a_{pt} and c_{pt} are much larger than the substrate lattice constant and the film needs to be quickly (in about 10 nm [21]) relaxed to accommodate that. The compressive stresses that remain after this relaxation should unlikely bring a_{pt} and c_{pt} closer to each other, as experiment demands, because they will compress further the already smaller c_{pt} axis, which is much more sensitive to the temperature changes [24] and is also expected to more readily accommodate the compression by increasing the octahedral tilts magnitude [44]. So, the average compressive strain, which is remnant after relaxation, seems unlikely to cause smaller splitting.

The more probable scenario of suppressing the around-the-normal domain tilts is the following. The domain tilts, which aim to fulfill the mechanical compatibility requirement, shall experience the counteraction from the torques arising across the material close to the substrate because the substrate does not intend to be tilted together with the domains. This way, the energy of twisting the material around the normal prevents the domain structure from reaching the mechanical compatibility that would be feasible in free-standing film.

A possible counterargument against this more probable scenario is that the twisted volume is small compared to the relaxed volume and should have relatively small impact on the energy. Another suspicion is that even if some force did, in fact, bring c_{pt} close to a_{pt} , such a structure is unlikely to sustain the AFE order parameter, since the smaller c_{pt} is required for accommodating octahedral tilts and the octahedral tilts appear to be essential for antiferroelectricity [7].

Keeping this in mind, our third approach seems particularly noteworthy, namely, that the absence of the expected splitting may be, in part, due to the coherence effect in the scattering of x rays by the nanodomain structure. Simulations show that such an effect can arise when domains are sufficiently small and sufficiently random in size, about 10 nanometers wide with the comparable magnitude of random spread. It is difficult to judge whether the films are indeed composed of such small domains. The available transmission electron microscopy studies of Chaudhuri *et al.* [21] and Si *et al.* [12]

show bigger individual AFE domains in film slices, 20–40 nm, but it is not so clear how representative those sizes are in the whole film volumes. Recent nanoscopic results indicate the smaller characteristic size of 13 nm [45].

These results call for attention toward previously reported reduced tilt-induced splitting in PbTiO₃/MgO films [46]. That case is different and apparently not yet well understood. The splitting there has been observed for those domains that are a minority in volume, while the majority appeared not tilted at all. Our mechanisms could be partially relevant there.

Summarizing those, the reduced splitting in PbZrO₃ films can be governed by a compromise between the energy of violating the mechanical compatibility and the energy of microtwists, and also due to the peculiarity of diffraction on nanodomain structures. The diffraction effect is unlikely to act alone because we see a clear difference in phase transitions as compared to bulk, which would be unlikely without the domains in the relaxed part of the film being under a considerable elastic influence.

It is probable that the appearance of in-plane M superstructures near the interface can help reduce the energy of microtwists.

V. CONCLUSION

Epitaxial PbZrO₃/SrRuO₃/SrTiO₃ heterostructures are promising in technologies, such as emerging ferroic memories, but they are also a good candidate for the model large-lattice-mismatched epitaxial ferroic. Most of the thin-film theories of ferroelectrics that rely on defect-free epitaxy, are very moderately applicable here, leaving the space largely empty from the predictive powered models. Our results demand an understanding of not only how the strain gets relaxed on going from the interface, which is largely understood [1], but also how the around-the-normal domain tilts, which arise from the pursuit of domain mechanical compatibility, get simultaneously relaxed going towards the interface. The tilt relaxation appears less effective than the strain relaxation as the tilts appear considerably smaller than those demanded by the zero-stress geometry. This conflict in domain mechanical compatibility should be among the factors changing the intrinsic behavior of lead zirconate, such as the unusual phase transitions observed in this work.

ACKNOWLEDGMENTS

The authors thank M. Jankowski, F. Carla, and H. Isern for their help with the experiment at ID03. R.G.B., M.A.K., and A.E.G. acknowledge the support of the Russian Science Foundation (Grant No. 20-72-10126) for the experimental work (apart from thin film synthesis) and interpretation (apart from first-principles analysis) and acknowledge G. Lityagin, D. Andronikova, I. Bronwald, A. Vakulenko, and S. Udovenko for supporting the preparation and conduction of the experiment.

[1] A. K. Tagantsev, L. E. Cross, and J. Fousek, *Domains in Ferroic Crystals and Thin Films* (Springer, New York, 2010).

[2] Z. I. Alferov, Nobel Lecture: The double heterostructure concept and its applications in physics, electronics, and technology, *Rev. Mod. Phys.* **73**, 767 (2001).

- [3] K. Redmond, Defect engineering increases polarization retention in ferroelectric thin films, *MRS Bull.* **45**, 254 (2020).
- [4] E. Gradauskaitė, K. A. Hunnestad, Q. N. Meier, D. Meier, and M. Trassin, Ferroelectric domain engineering using structural defect ordering, *Chem. Mater.* **34**, 6468 (2022).
- [5] R. G. Burkovsky, G. A. Lityagin, A. E. Ganzha, A. F. Vakulenko, R. Gao, A. Dasgupta, B. Xu, A. V. Filimonov, and L. W. Martin, Field-induced heterophase state in PbZrO₃ thin films, *Phys. Rev. B* **105**, 125409 (2022).
- [6] A. Tagantsev, K. Vaideeswaran, S. Vakhrushev, A. Filimonov, R. G. Burkovsky, A. Shaganov, D. Andronikova, A. Rudskoy, A. Baron, H. Uchiyama *et al.*, The origin of antiferroelectricity in PbZrO₃, *Nat. Commun.* **4**, 2229 (2013).
- [7] J. Íñiguez, M. Stengel, S. Prosandeev, and L. Bellaiche, First-principles study of the multimode antiferroelectric transition in PbZrO₃, *Phys. Rev. B* **90**, 220103(R) (2014).
- [8] J. Hlinka, T. Ostapchuk, E. Buixaderas, C. Kadlec, P. Kuzel, I. Gregora, J. Kroupa, M. Savinov, A. Klic, J. Drahokoupil *et al.*, Multiple Soft-Mode Vibrations of Lead Zirconate, *Phys. Rev. Lett.* **112**, 197601 (2014).
- [9] K. Boldyreva, D. Bao, G. Le Rhun, L. Pintilie, M. Alexe, and D. Hesse, Microstructure and electrical properties of (120) O-oriented and of (001) O-oriented epitaxial antiferroelectric PbZrO₃ thin films on (100) SrTiO₃ substrates covered with different oxide bottom electrodes, *J. Appl. Phys.* **102**, 044111 (2007).
- [10] L. Pintilie, K. Boldyreva, M. Alexe, and D. Hesse, Coexistence of ferroelectricity and antiferroelectricity in epitaxial PbZrO₃ films with different orientations, *J. Appl. Phys.* **103**, 024101 (2008).
- [11] R. Gao, S. E. Reyes-Lillo, R. Xu, A. Dasgupta, Y. Dong, L. R. Dedon, J. Kim, S. Saremi, Z. Chen, C. R. Serrao *et al.*, Ferroelectricity in Pb_(1+δ)ZrO₃ thin films, *Chem. Mater.* **29**, 6544 (2017).
- [12] Y. Si, T. Zhang, Z. Chen, Q. Zhang, S. Xu, T. Lin, H. Huang, C. Zhou, S. Chen, S. Liu *et al.*, Phase competition in high-quality epitaxial antiferroelectric PbZrO₃ thin films, *ACS Appl. Mater. Interfaces* **14**, 51096 (2022).
- [13] N. Pertsev and A. Zembilgotov, Energetics and geometry of 90 domain structures in epitaxial ferroelectric and ferroelastic films, *J. Appl. Phys.* **78**, 6170 (1995).
- [14] S. E. Reyes-Lillo and K. M. Rabe, Antiferroelectricity and ferroelectricity in epitaxially strained PbZrO₃ from first principles, *Phys. Rev. B* **88**, 180102(R) (2013).
- [15] K. Patel, S. Prosandeev, B. Xu, C. Xu, and L. Bellaiche, Properties of (001) NaNbO₃ films under epitaxial strain: A first-principles study, *Phys. Rev. B* **103**, 094103 (2021).
- [16] A. L. Roytburd, Modulated domain and heterophase structures in epitaxial layers due to solid-solid transformations, *MRS Online Proceedings Library (OPL)* **221**, 255 (1991).
- [17] N. A. Pertsev and V. G. Koukhar, Polarization Instability in Polydomain Ferroelectric Epitaxial Thin Films and the formation of Heterophase Structures, *Phys. Rev. Lett.* **84**, 3722 (2000).
- [18] W. Pompe, X. Gong, Z. Suo, and J. Speck, Elastic energy release due to domain formation in the strained epitaxy of ferroelectric and ferroelastic films, *J. Appl. Phys.* **74**, 6012 (1993).
- [19] S. Alpay, I. Misirliglu, V. Nagarajan, and R. Ramesh, Can interface dislocations degrade ferroelectric properties? *Appl. Phys. Lett.* **85**, 2044 (2004).
- [20] G. Catalan, B. Noheda, J. McAneney, L. J. Sinnamon, and J. M. Gregg, Strain gradients in epitaxial ferroelectrics, *Phys. Rev. B* **72**, 020102(R) (2005).
- [21] A. Roy Chaudhuri, M. Arredondo, A. Hähnel, A. Morelli, M. Becker, M. Alexe, and I. Vrejoiu, Epitaxial strain stabilization of a ferroelectric phase in PbZrO₃ thin films, *Phys. Rev. B* **84**, 054112 (2011).
- [22] G. Lityagin, D. Andronikova, I. A. Bronwald, M. Kniazeva, M. Jankowski, F. Carla, R. Gao, A. Dasgupta, A. Filimonov, and R. G. Burkovsky, Intermediate phase with orthorhombic symmetry displacement patterns in epitaxial PbZrO₃ thin films at high temperatures, *Ferroelectrics* **533**, 26 (2018).
- [23] G. A. Lityagin, A. F. Vakulenko, R. Gao, A. Dasgupta, A. V. Filimonov, and R. G. Burkovsky, Broadening of X-ray reflections and inhomogeneous strain distribution in PbZrO₃/SrRuO₃/SrTiO₃ epitaxial heterostructures, *J. Phys.: Conf. Ser.* **1236**, 012018 (2019).
- [24] R. W. Whatmore and A. M. Glazer, Structural phase-transitions in lead zirconate, *J. Phys. C: Solid State Phys.* **12**, 1505 (1979).
- [25] H. Fujishita and S. Hoshino, A study of structural phase-transitions in antiferroelectric PbZrO₃ by neutron-diffraction, *J. Phys. Soc. Jpn.* **53**, 226 (1984).
- [26] D. Corker, A. Glazer, J. Dec, K. Roleder, and R. Whatmore, A re-investigation of the crystal structure of the perovskite PbZrO₃ by x-ray and neutron diffraction, *Acta Crystallogr. Sect. B: Struct. Sci.* **53**, 135 (1997).
- [27] A. D. Bruce and R. A. Cowley, *Structural phase transitions* (Taylor and Francis, London, 1981).
- [28] M. A. Kniazeva, A. E. Ganzha, I. Jankowska-Sumara, M. Paściak, A. Majchrowski, A. V. Filimonov, A. I. Rudskoy, K. Roleder, and R. G. Burkovsky, Ferroelectric to incommensurate fluctuations crossover in PbHfO₃-PbSnO₃, *Phys. Rev. B* **105**, 014101 (2022).
- [29] B. Xu, O. Hellman, and L. Bellaiche, Order-disorder transition in the prototypical antiferroelectric PbZrO₃, *Phys. Rev. B* **100**, 020102(R) (2019).
- [30] A. Glazer, Simple ways of determining perovskite structures, *Acta Crystallogr., Sect. A* **31**, 756 (1975).
- [31] J. Ricote, D. Corker, R. Whatmore, S. Impney, A. Glazer, J. Dec, and K. Roleder, A TEM and neutron diffraction study of the local structure in the rhombohedral phase of lead zirconate titanate, *J. Phys.: Condens. Matter* **10**, 1767 (1998).
- [32] Z. An, H. Yokota, N. Zhang, M. Paściak, J. Fábry, M. Kopecký, J. Kub, G. Zhang, A. M. Glazer, T. R. Welberry, W. Ren, and Z. G. Ye, Multiple structural components and their competition in the intermediate state of antiferroelectric Pb(Zr,Ti)O₃, *Phys. Rev. B* **103**, 054113 (2021).
- [33] D. Viehland, D. Forst, and J.-F. Li, Compositional heterogeneity and the origins of the multicell cubic state in Sn-doped lead zirconate titanate ceramics, *J. Appl. Phys.* **75**, 4137 (1994).
- [34] S. B. Vakhrushev, D. Andronikova, I. Bronwald, E. Y. Koroleva, D. Chernyshov, A. V. Filimonov, S. A. Udovenko, A. I. Rudskoy, D. Ishikawa, A. Q. R. Baron *et al.*, Electric field control of antiferroelectric domain pattern, *Phys. Rev. B* **103**, 214108 (2021).
- [35] M. de Oliveira Guimarães, C. Richter, M. Hanke, S. Bin Anooz, Y. Wang, J. Schwarzkopf, and M. Schmidbauer, Ferroelectric phase transitions in tensile-strained NaNbO₃ epitaxial films probed by *in situ* x-ray diffraction, *J. Appl. Phys.* **132**, 154102 (2022).

- [36] E. J. Mittemeijer and U. Welzel, *Modern Diffraction Methods* (Wiley-VCH Verlag GmbH & Co. KGaA, Weinheim, Germany, 2013).
- [37] Y. U. Wang, Diffraction theory of nanotwin superlattices with low symmetry phase: Application to rhombohedral nanotwins and monoclinic M A and M B phases, *Phys. Rev. B* **76**, 024108 (2007).
- [38] D. W. Cooke, F. Hellman, J. Groves, B. Clemens, S. Moyerman, and E. Fullerton, Calorimetry of epitaxial thin films, *Rev. Sci. Instrum.* **82**, 023908 (2011).
- [39] Y. Yamada and T. Yamada, Inter-dipolar interaction in NaNO_2 , *J. Phys. Soc. Jpn.* **21**, 2167 (1966).
- [40] H. Terauchi, H. Takenaka, and K. Shimaoka, Structural phase transition in K_2SeO_4 , *J. Phys. Soc. Jpn.* **39**, 435 (1975).
- [41] C. J. de Pater and R. B. Helmholtz, Incommensurate structural phase transformation in Na_2CO_3 , *Phys. Rev. B* **19**, 5735 (1979).
- [42] R. G. Burkovsky, I. Bronwald, D. Andronikova, B. Wehinger, M. Krisch, J. Jacobs, D. Gambetti, K. Roleder, A. Majchrowski, A. Filimonov *et al.*, Critical scattering and incommensurate phase transition in antiferroelectric PbZrO_3 under pressure, *Sci. Rep.* **7**, 41512 (2017).
- [43] M. A. Knyazeva, D. Andronikova, G. Lityagin, I. A. Bronwald, P. Paraskevas, A. Majchrowski, K. Roleder, A. Filimonov, and R. G. Burkovsky, Phase transitions in lead hafnate under high pressure, *Phys. Solid State* **61**, 1759 (2019).
- [44] B. K. Mani, S. Lisenkov, and I. Ponomareva, Finite-temperature properties of antiferroelectric PbZrO_3 from atomistic simulations, *Phys. Rev. B* **91**, 134112 (2015).
- [45] J. E. Flores Gonzales, A. E. Ganzha, M. A. Kniazeva, D. A. Andronikova, A. F. Vakulenko, A. Filimonov, A. Rudskoy, C. Richter, A. Dasgupta, R. Gao *et al.*, Thickness independence of antiferroelectric domain characteristic sizes in epitaxial $\text{PbZrO}_3/\text{SrRuO}_3/\text{SrTiO}_3$ films, *J. Appl. Crystallogr.* **56**, 3 (2023).
- [46] K. Lee and S. Baik, Thickness dependence of domain formation in epitaxial PbTiO_3 thin films grown on MgO (001) substrates, *J. Appl. Phys.* **87**, 8035 (2000).